

# AC Power Theory From Poynting Theorem: Identification of the Power Components of Magnetic Saturating and Hysteretic Circuits

Francisco de León, *Senior Member, IEEE*, Layth Qaseer, and José Cohen

**Abstract**—This paper is the continuation of an earlier work on narrowing the theoretical gap with power theory (or “power definitions”) for nonlinear circuits. The underlying idea is to compute the active and reactive powers of a general single-phase circuit from only the knowledge of the instantaneous voltage and current at the circuit terminals. This is done to shed light on the long-standing controversy on the physical meaning of the various types of powers defined for nonsinusoidal waveforms. Previously, only the power components of nonlinear switching circuits consisting of constant resistive and inductive elements were properly identified. The method is now extended to be suitable for the identification of the power components of general single-phase nonlinear circuits including magnetic nonlinear components with saturation and hysteresis. The Poynting Theorem is applied to correctly identify the energy consumed in electrical elements (Joule losses) as well as the energy stored/restored and consumed in the hysteresis loop of magnetic elements. Numerous examples are presented for illustration and validation of the method.

**Index Terms**—Energy stored/restored, energy transformed, hysteresis losses, instantaneous power, nonlinear circuits, power definitions, power theory.

## I. INTRODUCTION

**T**HEORETICAL advances to the solution of the long-standing problem with “power definitions” for nonlinear circuits were presented in [1]. The underlying idea was to accurately identify the active and reactive power components of a generic load only from terminal measurements of the instantaneous voltage and current (see Fig. 1). The Poynting Theorem was used in [1] to accurately identify the elements of nonlinear switching loads consisting of linear  $R$ - $L$ - $C$  elements.

A number of published reviews of the important issues in the area of power definitions exist beginning with the 1920s [2], [3]. Some of the more recent ones giving interesting points of view, including the work and analysis of Emanuel [4], [5], Czarnecki [6], Willems [7], and Sutherland [8].

Manuscript received August 29, 2011; revised November 17, 2011; accepted February 15, 2012. Date of publication April 05, 2012; date of current version June 20, 2012. Paper no. TPWRD-00734-2011.

F. de León is with the Polytechnic Institute of New York University, Brooklyn, NY 11201 USA (e-mail: fdeleon@poly.edu).

L. Qaseer is with Polytechnic Institute of New York University, Brooklyn, NY 11201 USA, on leave from Al-Khwarizmi College of Engineering, University of Baghdad, Baghdad, Iraq (e-mail: lqaseer@poly.edu).

J. Cohen is with the Departamento de Ingeniería Eléctrica, División de Estudios de Posgrado, Universidad Nacional Autónoma de México (UNAM), 4510 México City, México (e-mail: jcohenmex@hotmail.com).

Color versions of one or more of the figures in this paper are available online at <http://ieeexplore.ieee.org>.

Digital Object Identifier 10.1109/TPWRD.2012.2188652

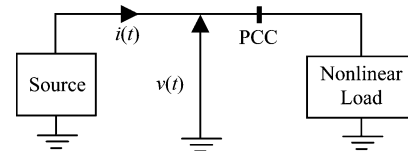


Fig. 1. General nonlinear load represented by a black box from the measurements of terminal instantaneous voltage and current.

The use of Poynting Theorem as the basis for understanding the power phenomena between a source and a load has been discussed in [8]–[12]. There are arguments in favor and against the use of the Poynting Theorem for the calculation of powers, but only in [1], a workable solution has been offered. The method in [1] is only applied to circuits containing constant  $R$ - $L$ - $C$  elements, where all nonlinearities are caused by the switching components.

In this paper, we extend the methodology proposed in [1] to include nonlinear magnetic circuits with saturation and hysteresis. Both the source and the load can be represented as black boxes since only the information of the instantaneous voltage and current at the point of common coupling (PCC) is needed to properly identify the power components of the load by computing the power and energy transferred in the line as shown in Fig. 1.

The method proposed in [1] was derived from the Poynting Theorem, describing the transfer of power and energy between a source and a load. When Poynting Theorem is applied to electrical circuits, it takes the following form:

$$\text{power transferred}(t) = \text{power transformed}(t) + \frac{d}{dt}[\text{energy stored/restored}(t)] \quad (1)$$

which was interpreted in [1] as follows:

$$p(t) = a(t) + r(t) \quad (2)$$

where  $a(t)$  is the instantaneous active power and  $r(t)$  is the instantaneous reactive power.

In [1], a one-to-one relationship between the time variations of the energy stored/restored and reactive power was assumed. Very good results were obtained from (2) when applied to nonlinear switching circuits composed of linear  $R$ - $L$ - $C$  elements. The nonlinearities were caused only by the switching devices. We note, however, that while (1) is correct, the interpretation given in (2) is not. This is so because the actions of storing and restoring energy are not necessarily perfectly efficient as was assumed in (2). Consequently, since in the process of storing

and restoring energy there could be losses not considered in (2), the method needs to be expanded to account for the hysteresis losses.

In this paper an improvement to the method of [1] is presented to properly treat general single-phase circuits with all kinds of nonlinearities including saturation and (both electric and magnetic) hysteresis. The equivalent circuit of a hysteretic load takes the shape of the Steinmetz equivalent circuit [13] commonly used for induction motors and transformers; therefore, offering a better understanding of the mechanism of core loss in machines.

This paper also presents an equivalent circuit with full physical meaning for hysteretic inductors (representing the magnetizing effects of machines: generators, transformer, motors, etc.) using a parallel  $R$ - $L$  circuit. In addition, this paper offers a methodological way to distinguish (or separate) the Joule loss from the hysteresis loss in a load only from the analysis of the power and energy transferred to the load through the circuit terminals.

In a sequel paper, we will present the practical engineering aspects, such as measurement techniques and associated instrumentation; revenue metering; power factor, including practical and economic consequences; and compensation procedures.

## II. POYNTING THEOREM AND HYSTERESIS LOSS

The Poynting Theorem was published in 1884 [14]. In its most general form, applied to include nonlinear and hysteretic media, it can be written as

$$\oint_S \vec{E} \times \vec{H} \cdot d\vec{S} = - \int_V \vec{E} \cdot \vec{J} dV - \frac{\partial}{\partial t} \int_V \frac{1}{2} \left( \int \vec{E} \cdot d\vec{D} \right) dV - \frac{\partial}{\partial t} \int_V \frac{1}{2} \left( \int \vec{H} \cdot d\vec{B} \right) dV. \quad (3)$$

The term on the left-hand side is the total power transferred. The first term on the right-hand side is Joule's Law representing the power transformed into heat by the circulation of electric current in the circuit. The second term on the right-hand side describes the changes (with time) of the energy store/restore process in the electric field. The last term is the time variation of the energy stored/restored in the magnetic field. The integrals

$$\int \vec{E} \cdot d\vec{D} \quad \text{and} \quad \int \vec{H} \cdot d\vec{B} \quad (4)$$

describe the energy density store/restore process for nonlinear media, including saturation and hysteresis.  $D$  and  $E$ , along with  $B$  and  $H$  are not necessarily related through a single value (permittivity or permeability) scalar or a single-valued function. When hysteresis is present, (4) is used to compute the losses in the cycle.

Take, for example, the magnetic term in (4) applied to a nonlinear (saturable) inductor represented by two lines in Fig. 2(a). The integral corresponds to the shaded area. As the fields vary with time, the energy density storing process and energy density restoring process paths follow the same curve described by the  $B$ - $H$  relationship [Fig. 2(a)]. Therefore, the integration process gives the same area under the curve (during the store/restore process). Under those conditions, all energy that is stored

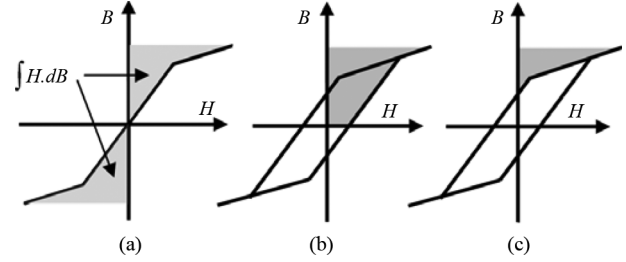


Fig. 2. (a) Energy stored/restored in a nonlinear (nonhysteretic) inductor represented by two straight lines. (b) Energy stored in a hysteretic inductor. (c) Energy restored by a hysteretic inductor.

is eventually restored, producing a 100% efficient process characteristic of an ideal inductor (whether it is linear or nonlinear). The sole requirement is that  $H$  and  $B$  be related by a single valued permeability ( $B = \mu H$ ) or a single-valued function of the type  $B = \mu(B)H$ .

The energy store/restore process for a hysteretic inductor is also presented in Fig. 2. Fig. 2(b) shows the energy density store process starting from  $B = 0$  to  $B = B_{\max}$ . Fig. 2(c) shows the energy density that is restored to the source when  $B$  reduces from  $B_{\max}$ . One can notice that in this case, the process is not perfectly efficient. Not all energy stored is restored; some energy is lost in the hysteresis loop. The heat dissipating mechanism is quite different from that of Joule's losses. The hysteresis losses are caused by friction between magnetic domains during the realignment process [15]. It is known that the hysteresis energy density losses are equal to the area of the hysteresis loop [12], [15], which is mathematically expressed by (4) when performing the integrals over a period.

Piece-wise linear approximations have been used in this paper to represent saturation and hysteresis. This is done because a linear behavior helps explaining the concepts. In addition, linear approximations give the possibility of quickly identifying the correctness of the results. Reference [12] offers a clear explanation of the hysteresis-loss mechanism using piece-wise linear approximations.

Equation (3), when applied to electrical circuits containing hysteretic components, can be written as follows:

$$p(t) = p_e(t) + p_m(t) \quad (5)$$

where  $p_e(t)$  is the electric power and  $p_m(t)$  is the magnetic power. The electric power  $p_e(t)$  can have up to three components: The first corresponds to the power consumed in the system as heat by Joule's Law (volume integral of  $\vec{E} \cdot \vec{J}$ ); The second component is the electric hysteresis loss given by the dielectric losses commonly known as  $\tan(\delta)$ ; The third component is due to the perfect dielectric energy store/restore process ( $\vec{E} \cdot \vec{D}$ ) (i.e., the capacitive reactive power). This is expressed as

$$p_e(t) = a_J(t) + a_{He}(t) + r_C(t) \quad (6)$$

where  $a_J(t)$  is the Joule power,  $a_{He}(t)$  is the electric hysteresis loss, and  $r_C(t)$  is the capacitive reactive power. Note that we have used the symbol  $a$  (= active power) for the Joule loss  $a_J(t)$  and the electric hysteresis loss  $a_{He}(t)$  since those components

are elements of the total active power (representing the energy transformed or consumed). The capacitive reactive power  $r_C(t)$  is due to the ideal energy store/restore process ( $\vec{E} \cdot \vec{D}$ ). We make the remark that capacitive loads are uncommon in real-life low-voltage circuits. The capacitive power is considered in this paper only to give generality to the presented methodology.

The magnetic power  $p_m(t)$  can have two components: 1) the magnetic hysteresis loss component  $a_{Hm}(t)$  and 2) the inductive reactive power  $r_L(t)$  due to the ideal energy store/restore process ( $\vec{H} \cdot \vec{B}$ ). Thus, we have

$$p_m(t) = a_{Hm}(t) + r_L(t). \quad (7)$$

Equation (3) can also be written as

$$\begin{aligned} p(t) &= \text{Joule power}(t) + \text{hysteresis loss}(t) \\ &\quad + \text{reactive power}(t) \\ p(t) &= a_J(t) + [a_{He}(t) + a_{Hm}(t)] + [r_C(t) + r_L(t)] \\ p(t) &= a_J(t) + a_H(t) + r(t) \\ p(t) &= a(t) + r(t). \end{aligned} \quad (8)$$

Equation (8), different from (1), lumps all energy transformed (including that due to changes in the stored energy) in the active power term  $a(t)$ . Only reactive power from the ideal store/restore process is contained in  $r(t)$ .

The power quantities of (8) have the following properties:  $a_J(t)$ ,  $a_{He}(t)$ , and  $a_{Hm}(t)$  represent energy consumed or lost in the circuit. Therefore, at all times, they are positive or zero. The sum  $a(t) = a_J(t) + a_H(t)$ , where  $a_H(t) = a_{He}(t) + a_{Hm}(t)$  is the total power consumed at every instant. Therefore, its integral over a cycle must be equal to the average active power  $P$ . The reactive power  $r(t) = r_C(t) + r_L(t)$  and each of its components represent the ideal energy store/restore process and have zero average. These conditions are expressed mathematically as

$$\begin{aligned} a_J(t) &\geq 0; & a_{He}(t) &\geq 0; & a_{Hm}(t) &\geq 0; \\ a_H(t) &\geq 0; & a(t) &\geq 0 \end{aligned} \quad (9)$$

$$\begin{aligned} w(t) &= \int v(t)i(t)dt = \int p(t)dt \\ &= \int [a_J(t) + a_H(t) + r(t)] dt \end{aligned} \quad (10)$$

$$\begin{aligned} \frac{1}{T} \int_0^T v(t)i(t)dt &= \frac{1}{T} \int_0^T [a_J(t) + a_H(t)]dt \\ &\quad + \frac{1}{T} \int_0^T [r(t)]dt = P. \end{aligned} \quad (11)$$

Since

$$\frac{1}{T} \int_0^T [r(t)]dt = 0 \quad (12)$$

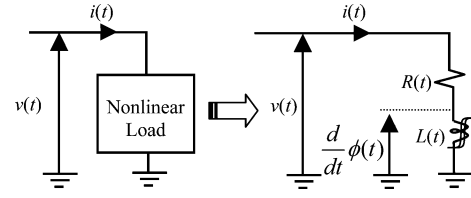


Fig. 3. Series equivalent circuit for a nonlinear load.

the following condition must also be met:

$$\frac{1}{T} \int_0^T a_H(t)dt = \text{Area of the hysteresis loop}. \quad (13)$$

Equations (9)–(13) do not participate in the identification of powers, but they can be used to verify that the identification method proposed in this paper works correctly.

### III. POWER IDENTIFICATION OF ELECTRIC CIRCUITS CONTAINING HYSTERETIC COMPONENTS

To build on our previous work [1], we start the power identification algorithm by separating the Joule power  $a_J(t)$  from the power due to the store/restore process. The latter,  $d/dt[w_{SR}(t)]$ , includes the power consumed (or transformed) in the process plus the changes with time of the reactive energy due to the store/restore process. Combining (1) and (8), we can write the following expression:

$$\begin{aligned} p(t) &= a_J(t) + [a_{He}(t) + a_{Hm}(t) + r_C(t) + r_L(t)] \\ p(t) &= \text{Joule power}(t) + \frac{d}{dt} [\text{energy stored/restored}(t)] \\ p(t) &= a_J(t) + \frac{d}{dt} w_{SR}(t). \end{aligned} \quad (14)$$

Previously, we obtained a numerical procedure that successfully identifies and separates the resistive and inductive powers from the total (instantaneous) power. Although practical loads are always inductive, in [1], it was demonstrated that the same method can be used when the load is capacitive by computing the capacitance from

$$C(t) = \frac{\int i(t)dt}{L(t) \frac{di(t)}{dt}}. \quad (15)$$

Equation (14) can be seen as originating from an equivalent series  $R$ – $L$  circuit composed by a time-varying resistor  $R(t)$  and a time-varying inductor  $L(t)$  as shown in Fig. 3. The resistor represents the Joule power, while the hysteretic inductor includes the losses in the store/restore process as well as the reactive power. We can write the Kirchhoff's Voltage Law (KVL) applied to the series model as

$$v(t) = R(t)i(t) + \frac{d}{dt} \phi(t) = R(t)i(t) + \frac{d}{dt} [L(t)i(t)]. \quad (16)$$

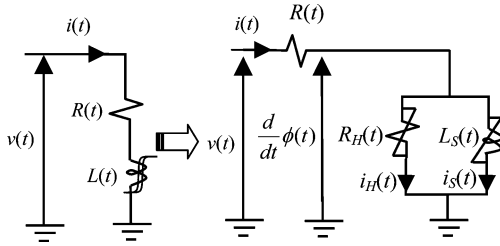


Fig. 4. Equivalent circuit for a nonlinear hysteretic load.

In terms of power, (16) can be written as

$$p(t) = v(t)i(t) = R(t)i^2(t) + i(t)\frac{d}{dt}[L(t)i(t)]. \quad (17)$$

We remark that, in practice, the instantaneous voltage and current at the PCC (see Fig. 1) are obtained from analog-to-digital converters (ADCs) running at a fixed sampling rate. Therefore, the power and energy at a particular point in time  $t_k = k\Delta t$  are computed from

$$p(t_k) = v(t_k)i(t_k) \quad (18)$$

and

$$w(t_k) = \int_{t_k}^{t_k+\Delta t} p(t)dt = \int_{t_k}^{t_k+\Delta t} v(t)i(t)dt. \quad (19)$$

When the sampling frequency is sufficiently fast, the resistance  $R(t)$  and inductance  $L(t)$  can be treated as constant between samples; say, from  $t_k$  to  $t_k + \Delta t$ . Therefore,  $R(t_k)$  and  $L(t_k)$  can be taken out of the derivative and integral signs in (16) and (17). Thus, to identify the equivalent inductive and resistive elements of the circuit of Fig. 3, the following matrix equation needs to be solved at each time  $t_k$ [1]

$$\begin{bmatrix} i(t_k)^2 & i(t_k)\frac{d}{dt}i(t)|_{t=t_k} \\ \int_{t_k}^{t_k+\Delta t} i(t)^2 dt & \int_{t_k}^{t_k+\Delta t} i(t)\frac{d}{dt}i(t)dt \end{bmatrix} \begin{bmatrix} R(t_k) \\ L(t_k) \end{bmatrix} = \begin{bmatrix} p(t_k) \\ w(t_k) \end{bmatrix}. \quad (20)$$

Recall that  $R(t_k)$  only represents the resistance due to Joule effect power  $a_J(t)$ .  $L(t_k)$  in (20) gives the total magnetic power  $p_m(t)$  that contains the information of the active power (hysteresis losses)  $a_H(t)$  and the reactive power  $r(t)$  in the inductor as  $p_m(t) = a_H(t) + r(t)$ .

The separation of the hysteresis power losses and the reactive power is done by recognizing that a hysteretic inductor should be modeled as a parallel circuit containing a nonlinear (saturating, but not hysteretic) inductor  $L_S(t)$  and a nonlinear resistor  $R_H(t)$  as shown in Fig. 4. For this, we need to compute the (internal) flux first. By inspection of the circuit of Fig. 3, we obtain

$$\frac{d}{dt}\phi(t) = v(t) - R(t)i(t). \quad (21)$$

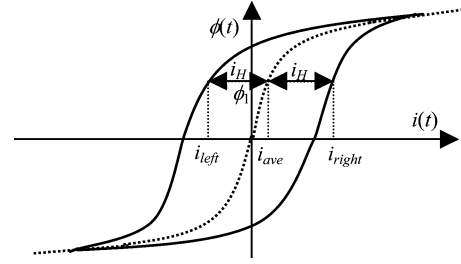


Fig. 5. Calculation of the saturation (no-loss) curve from the hysteresis loop.

The instantaneous flux is obtained from the numerical integration of (21) yielding

$$\phi(t_k + \Delta t) = \phi(t_k) + \int_{t_k}^{t_k+\Delta t} [v(t) - R(t)i(t)] dt. \quad (22)$$

Note that the initial flux  $\phi(t_k)$  for  $t = k = 0$ ,  $\phi(t_0) = \phi_0$  is yet unknown. To start the process, the integral in (22) can be performed by assuming an initial value; for convenience, we take  $\phi_0 = 0$ . The actual value of  $\phi_0$  can be computed by realizing that the average flux must be zero for periodic operating conditions. (The initial flux needs to be equal to the final flux in a cycle.) This is expressed mathematically as

$$\overline{\phi(t)} = 0 = \frac{1}{T} \int_0^T \phi(t)dt + \phi_0 = \frac{1}{T} \sum_{k=1}^N \phi(t_k)\Delta t + \phi_0. \quad (23)$$

Therefore, we obtain

$$\phi_0 = -\frac{1}{T} \sum_{k=1}^N \phi(t_k)\Delta t. \quad (24)$$

$\phi_0$  in (24) should be added to all values of  $\phi(t_k)$  in (22) to remove the dc bias given by assuming  $\phi_0 = 0$ .

By plotting the curve of  $\phi(t)$  versus  $i(t)$ , one can easily identify whether the equivalent inductor  $L(t)$  is hysteretic (has losses) or not. If the resulting plot is a single-valued curve, then there are no hysteresis losses and the identification process ends with the solution of (20). The presence of hysteresis produces a  $\phi(t)$  versus  $i(t)$  curve that has an internal area. To separate the power losses from reactive power, we need to compute the saturation single-valued curve. Consider the hysteresis loop depicted in Fig. 5. Let us take a horizontal line at  $\phi_1$  and call the current on the right-hand side of the cycle  $i_{right} = i(t_{right})$ , when the current is increasing, and the current on the left-hand side as  $i_{left} = i(t_{left})$  when the current is decreasing. The saturation (lossless) curve corresponds to the curve of the average between the two currents for the same flux  $\phi_1$  in the cycle given by

$$i_S = i_{ave} = \frac{(i_{right} + i_{left})}{2}. \quad (25)$$

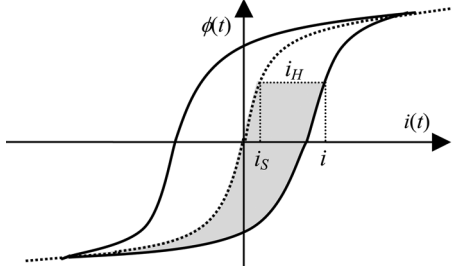


Fig. 6. Calculation of the hysteresis losses from the flux versus current curve.

The hysteresis current is given by (see Fig. 5)

$$i_H(t) = \begin{cases} i_{\text{right}} - i_S(t_{\text{right}}) \\ i_{\text{left}} - i_S(t_{\text{left}}) \end{cases} = i(t) - i_S(t). \quad (26)$$

The instantaneous losses consumed by the hysteretic inductor are computed from the hysteresis current with the following expression:

$$a_H(t) = [i_H(t)] \frac{d}{dt} \phi(t) = [i(t) - i_S(t)] \frac{d}{dt} \phi(t) \quad (27)$$

where  $i_H(t)$  and  $i_S(t)$  are obtained from the hysteresis and saturation curves (from (25) and (26)) and  $d\phi(t)/dt$  from (21). The (lossless) reactive power  $r(t)$  can be computed from the following expression:

$$r(t) = i_S(t) L_S(t) \frac{d}{dt} i_S(t). \quad (28)$$

In addition to the identification of the power components of a general load from the terminal measurements, our methodology given in (21)–(28) can be used to determine a (physically sound) equivalent circuit of a hysteretic inductor; see Fig. 4. The series resistor  $R(t)$ , in general, represents the energy that is transferred to a load plus the Joule losses. For a circuit consisting only of a hysteretic inductor it represents the losses in the winding resistance and is computed directly from (20); the saturating (but nonhysteretic inductor)  $L_S(t)$  represents the lossless energy process and is computed taking the derivatives of (22) and (25) as follows:

$$L_S(t_k) = \frac{\frac{d\phi(t_k)}{dt}}{\frac{di_S(t_k)}{dt}} = \frac{d\phi(t_k)}{di_S(t_k)}. \quad (29)$$

We note that, as expected, both expressions in (29) yield the same numerical results. The nonlinear shunt resistor  $R_H(t)$  represents the hysteresis losses and can be computed from (26) and (27) as

$$R_H(t_k) = \frac{a_H(t_k)}{i_H^2(t_k)} = \frac{\frac{d\phi(t_k)}{dt}}{i_H(t_k)}. \quad (30)$$

As before, with (29), both expressions in (30) give the same numerical result.

Note that in practice it is not possible to apply sufficiently high voltages to electrical equipment to find the entire magnetizing (or hysteresis) curve by measurement. We remark,

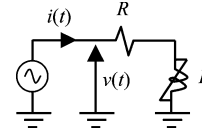


Fig. 7. Sinusoidal source feeding a linear resistor in series with a nonlinear (saturating) inductor.

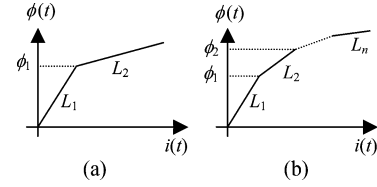


Fig. 8. Nonlinear (saturating) inductors represented by linear piecewise approximations. (a) Two lines. (b)  $n$ -lines.

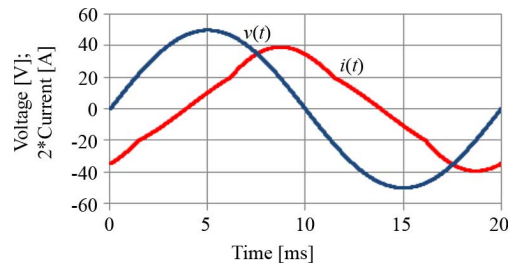


Fig. 9. Voltage and current for the circuit of Fig. 7 with the saturation curve of Fig. 8(a).

however, that the knowledge of the magnetizing curve is not a requisite for the application of our method. We only need to measure the terminal voltage and current of the load to be able to compute its instantaneous active and reactive power at the operating point. With our method, one can find the saturation (or hysteresis) curve up to the point at which the device is operating.

#### IV. EXAMPLES

The applicability of the method to general nonlinear single-phase circuits will be demonstrated by gradually increasing the complexity of the load, whose power components are to be identified. To start the study, the simple circuit shown in Fig. 7 is used. It consists of a linear resistor in series with a nonlinear saturating (nonhysteretic) inductor.

##### A. Approximation of Saturation by Two Lines

The first example consists of a variable inductor represented by two straight lines and is shown in Fig. 8(a); the negative part is symmetric. The 50-Hz voltage and current are shown in Fig. 9 for the following parameters:  $R = 1 \Omega$ ,  $L_1 = 10$  mH,  $L_2 = 5$  mH,  $\phi_1 = 0.1$  Wb. The flux and current have been computed by simulation in two ways: 1) using the EMTP-RV [16] and 2) solving the nonlinear differential equation by direct integration (trapezoidal rule of integration) with our own Matlab code. In both cases, the simulations ran until steady state was reached yielding identical results.

After the application of the identification process, for  $R_k$  and  $L_k$ , given in (20), we get the results of Fig. 10. One can appreciate that for this simple circuit, the method very accurately computes the original parameters ( $R$ ,  $L_1$ , and  $L_2$ ) only from the information of the instantaneous voltage and current at the

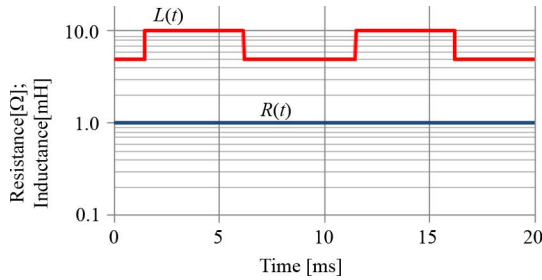


Fig. 10. Results of the identification process (20) for the voltage and current of Fig. 9.

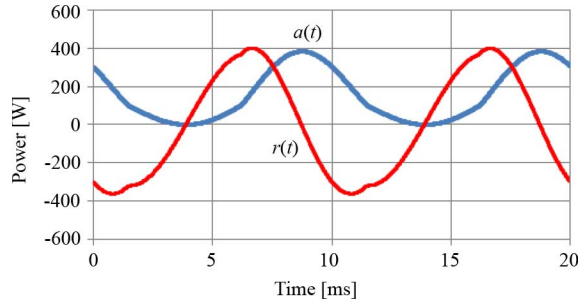


Fig. 11. Instantaneous active and reactive powers for the circuit of Fig. 7 with the saturation curve of Fig. 8(a).

circuit terminals. For more complex circuits, only the instantaneous values of the equivalent resistances and inductances can be computed, which yields the same instantaneous active and reactive power components than the entire circuit components. Fig. 11 shows the instantaneous active and reactive powers  $a(t)$  and  $r(t)$ , respectively. As expected, the instantaneous active power is equal to or greater than zero at all times, and the reactive power has zero average.

In several of the equivalent resistances, inductances, and active and reactive powers, very-high-frequency oscillations (or spikes) show when the change of values occur. However, this presents no practical implementation problems since the oscillations can be eliminated very easily with a numerical filter. A simple filter based on the derivative of the signal was successfully implemented in this paper. In not one of the examples did we need to apply a more sophisticated filter to obtain a clean figure.

#### B. Approximation of Saturation by Five Lines

The second example consists of an inductor with five linear sections. The value of the inductors is given in Table I and we use  $R = 1 \Omega$ . Fig. 12 shows the results of the identification process. Once again, one can see that the method is very effective in identifying the original circuit parameters ( $R = 1 \Omega$ ;  $L = 5, 10, 20, 40,$  and  $60$  mH). Fig. 13 shows the instantaneous active and reactive powers  $a(t)$  and  $r(t)$ . As before,  $a(t) \geq 0$  and  $r(t) = 0$ .

#### C. Approximation of Saturation by $N$ -lines

A real saturating inductor, whose core is made of transformer steel M4, was represented by a piecewise linear approximation with 50 lines. We have confirmed that the method properly identifies each section (results not shown due to a lack of space).

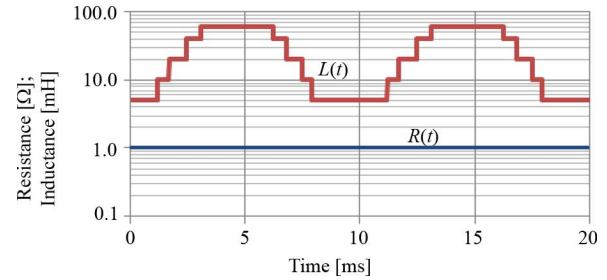


Fig. 12. Results of the identification process (20) with a resistor  $R = 1 \Omega$  and a linear-pieewise inductor.

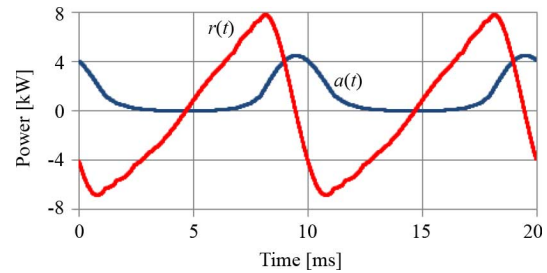


Fig. 13. Instantaneous active and reactive powers for the circuit of Fig. 7 with the saturation curve of Fig. 8(b) using five linear sections.

TABLE I  
INDUCTANCE VALUES FOR A LINEAR PIECEWISE APPROXIMATION OF A SATURATING INDUCTOR WITH FIVE LINES

$n$	$\phi_n$	$L_n$ [mH]
1	0.60	60
2	0.80	40
3	1.00	20
4	1.10	10
5	1.15	5

In all previous examples, the flux versus current curves have been single-valued functions. Therefore, all magnetic energy store/restore processes are carried out with 100% efficiency. Next, we show hysteretic examples.

#### D. Circuit With a Hysteretic Inductor

The next example consists of the application of the identification technique to the circuit of Fig. 7 for a hysteretic inductor. The flux versus current curve of the inductor is represented by a piecewise linear loop as shown in Fig. 14. A simple two-line piecewise model has been chosen in order to validate the results by inspection. From the figure, we can recognize four points with coordinates given in Table II. The curve is characterized by two slopes

$$L_1 = \frac{0.6 - 0.4}{10 - 2} = 25 \text{ [mH]};$$

$$L_2 = \frac{0.6 + 0.4}{10 + 2} = 83.3 \text{ [mH]}. \quad (31)$$

Fig. 15 shows the results of the identification process of (20). Note that the two inductance values are exactly the slopes of the two straight lines forming the hysteresis loop in Fig. 14. As before, we have confirmed that  $R(t) = 1 \Omega$  for all  $t$  (results not shown). Therefore, once again, one can note that the method is effective in identifying the original  $R(t)$  and  $L(t)$  parameters.

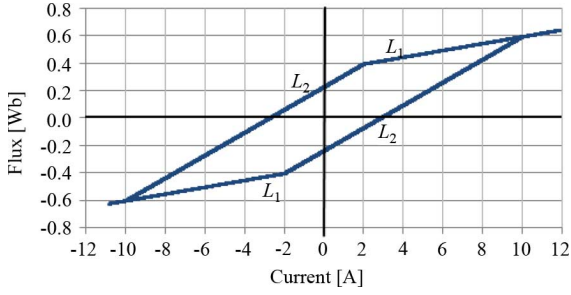


Fig. 14. Linear piecewise approximation of a hysteresis loop with four sections.

TABLE II  
FLUX VERSUS CURRENT VALUES FOR THE LINEAR PIECEWISE APPROXIMATION OF THE HYSTERETIC INDUCTOR OF FIG. 14

Point	$\phi_k$	$i_k$
1	0.6	10.0
2	0.4	2.0
3	-0.6	-10.0
4	-0.4	-2.0

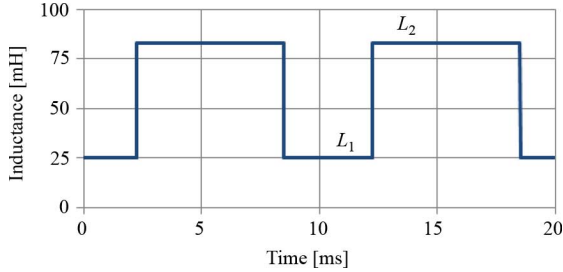


Fig. 15. Results of the identification process (20) applied to a hysteretic inductor. The inductance values are identified correctly.

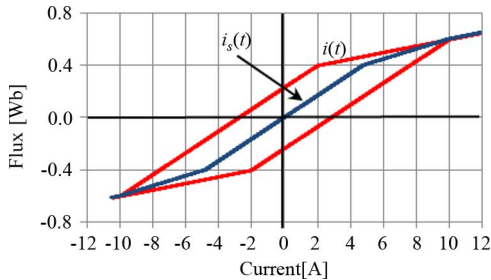


Fig. 16. Flux versus current plot and calculation of the lossless saturation curve.

Note, however, that at this point, we have only identified the Joule power loss  $a_J(t) = R(t)i(t)^2$  and the variations of the energy stored (or magnetic power) given by  $p_m(t) = a_H(t) + r(t) = i(t)L(t)[di(t)/dt]$ .

To separate the hysteresis loss  $a_H(t)$  and the reactive power  $r(t)$  from  $p_m(t)$ , we follow the procedure established in (21)–(28). The flux versus current plot, including the average (lossless) saturation curve, is shown in Fig. 16, which was obtained from (21) and (22) and the process given in Fig. 5.

Fig. 17 shows the terminal current  $i(t)$ , the obtained hysteresis current  $i_H(t)$ , and lossless current  $i_S(t)$ . One can appreciate that while the terminal current  $i(t)$  does not have odd symmetry, the lossless current  $i_S(t)$  is symmetric (about the

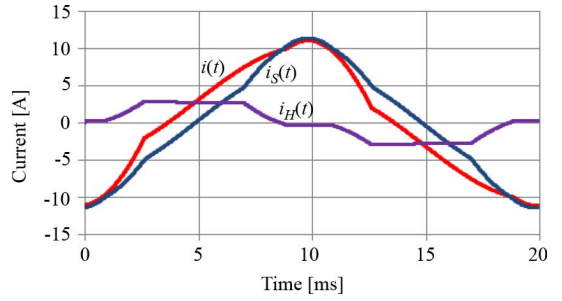


Fig. 17. Results of the separation of currents into saturation and hysteresis currents as in Fig. 5.

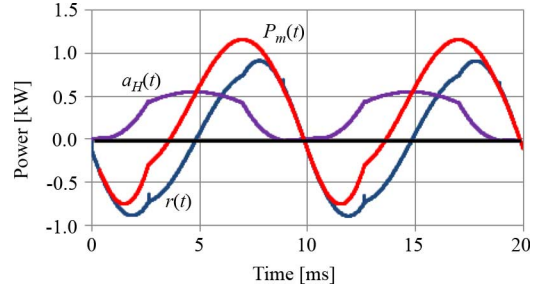


Fig. 18. Instantaneous magnetic power  $p_m(t)$ , reactive power  $r(t)$ , and hysteresis loss  $a_H(t)$  for the circuit of Fig. 3 with the hysteresis loop of Fig. 14.

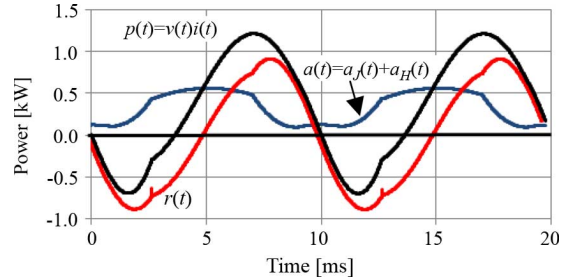


Fig. 19. Results of identifying the active and reactive powers from the total power for a series circuit including a hysteretic inductor.

10-ms line). The hysteresis current  $i_H(t)$  for this case exists only when hysteresis losses are produced. This happens only when  $i_{right} \neq i_{left} \neq i_{ave}$  is in the loop. The hysteresis current is zero in the top and bottom regions of the hysteresis loop where the three curves coincide. In those regions,  $i(t) = i_S(t)$  and there are no hysteresis losses.

Fig. 18 shows the magnetic power components that have been identified. We note that the total magnetic power has been divided into hysteresis loss and reactive power as  $p_m(t) = a_H(t) + r(t)$ . While the average of  $p_m(t)$  is not zero since it contains losses, the average of the reactive power  $r(t)$  is zero. We also note that  $a_H(t)$  is positive or zero at all times.

Fig. 19 shows the separation of the total power into its active and reactive power components as  $p(t) = a(t) + r(t)$ . The active power has two components  $a(t) = a_J(t) + a_H(t)$ . We note that, consistent with physical reality, the loss component  $a(t) > 0$  at all times while the average of  $r(t)$  is zero.

### E. General Nonlinear Circuit (Saturation and Hysteresis)

In this section, the identification of the power components of a circuit with two nonlinear branches is performed. The circuit

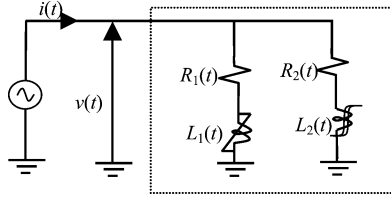


Fig. 20. Two-branch nonlinear circuit to be identified only from terminal measurements.

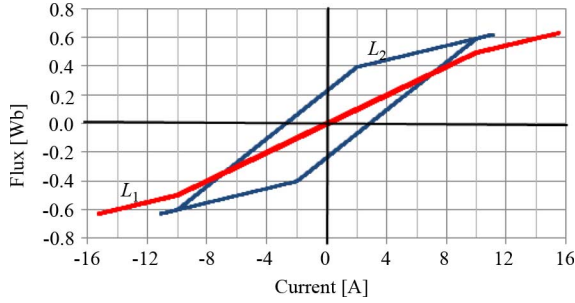


Fig. 21. Flux versus current curves for the inductors of the two-branch nonlinear circuit of Fig. 20.

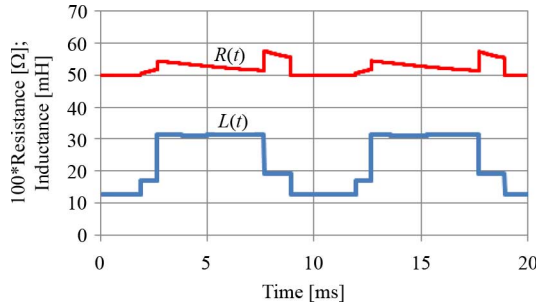


Fig. 22. Equivalent resistance and inductance after the identification process.

is illustrated in Fig. 20. One of the branches is hysteretic and the other has only saturation. Fig. 21 shows the flux versus current curves of the two inductors. The values of  $L_1$  are 50 and 25 mH before and after the knee, respectively. The values for  $L_2$  are given in Table II. The resistors on each branch are 1  $\Omega$ .

The results of the identification process are shown in Fig. 22. One can appreciate that the method effectively identifies the resistive (Joule effect) and inductive (store/restore) power components. When the two branches are operating in a linear region, the equivalent resistor is 0.5  $\Omega$ , which is the parallel of the two 1- $\Omega$  resistors. The value changes as the flux enters a new region. From the computed equivalent inductance, one can distinguish four values: 12.5, 16.67, 19.23, and 31.25 mH, which correspond to the parallel combinations of the different inductances (50 and 25 mH with 25 and 83.3 mH) of Fig. 21.

Fig. 23 shows the equivalent hysteretic inductor of the parallel circuit, together with the average single-value (lossless) inductor. One can see that the equivalent inductor has a narrower hysteresis looking cycle than  $L_2$ . However, the identified inductor has the same area as  $L_2$ , which is responsible for all hysteresis losses in the circuit under analysis.

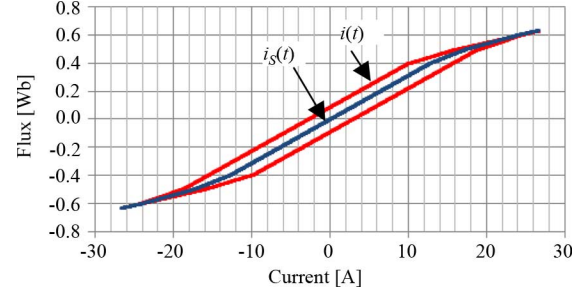


Fig. 23. Identified flux versus current equivalent hysteresis cycle and average saturation curve.

As before, the method of this paper can successfully identify the elements of the general equivalent circuit of Fig. 4. From the knowledge of the terminal measurements  $v(t)$  and  $i(t)$ , plus the calculated variables  $R(t)$ ,  $L_S(t)$ ,  $i_S(t)$ , and  $i_H(t)$ , the power components can be computed by

$$\begin{aligned} a(t) &= a_J(t) + a_H(t) \\ &= R(t)i^2(t) + i_H(t)[v(t) - R(t)i(t)] \\ r(t) &= i_S(t)L_S(t)\frac{d}{dt}i_S(t). \end{aligned} \quad (32)$$

#### F. Discussion

The result of the power identification process is always an equivalent circuit as the one depicted in Fig. 4. Three elements, with distinct energetic characteristics, are identified as  $R(t)$ ,  $R_H(t)$ , and  $L_S(t)$ .  $R(t)$  accounts for the Joule loss,  $L_S(t)$  represents the ideal energy store/restore process, and  $R_H(t)$  considers the (hysteresis) energy losses incurred during the store/restore cycle. Not all three elements exist for a particular case; one or two could be zero (examples are not shown, but we verified this statement to be true).

If two circuits with different topology have exactly the same terminal performance (say the same instantaneous terminal voltage and current at every time), then from the Poynting Theorem viewpoint (energy transferred between the source and the load), the two circuits are indistinguishable. They both would have the same parameters in the equivalent circuit. In practice, this situation is virtually impossible (because no two loads could be identical), but theoretically speaking, one could design two different circuits to perform identically and our method could not tell them apart. This, however, should not be seen as a limitation of the method. The reality is that both circuits would consume and store/restore energy in exactly the same way and, therefore, they must have the same equivalent circuit. As such, the method does not identify the actual elements of a composite load, but it obtains an equivalent circuit that consumes and stores energy in exactly the same way as the composite load.

#### V. CONCLUSION

In this paper, a methodology and an equivalent circuit have been proposed for the identification of the power components of general (periodic excitation) single-phase circuits. Only the

knowledge of the instantaneous current and voltage at the terminals is needed to fully characterize the power phenomena. The equivalent circuit consists of a resistor, representing the Joule losses, which is in series with a parallel  $R$ - $L$  circuit, representing the hysteresis active power losses and the reactive power, respectively.

The identification method has been applied successfully for the recognition of nonlinear single-phase circuits, including saturating and hysteretic inductors. A number of examples with different levels of complexity have been presented for illustration and validation of the method.

This paper contributes to close the long-standing theoretical gap with power definitions for single-phase nonlinear circuits. Since the derived power quantities are in perfect agreement with the Poynting Theorem, they offer incontestable physical meaning.

We intend to continue working on the practical engineering aspects of the method (e.g., instrumentation, revenue metering, power factor, and compensation procedures) and the application to three-phase unbalanced circuits.

#### REFERENCES

- [1] F. de León and J. Cohen, "AC power theory from Poynting Theorem: Accurate identification of instantaneous power components in nonlinear-switched circuits," *IEEE Trans. Power Del.*, vol. 25, no. 4, pp. 2104–2112, Oct. 2010.
- [2] Preliminary Report of the Special Joint Committee, Power Factor in Polyphase Circuits, AIEE Trans. 1920, pp. 1449–1450.
- [3] A. E. Knowlton, "Reactive power concepts in need of clarification," *AIEE Trans.*, vol. 52, pp. 744–747, Sep. 1933.
- [4] A. E. Emanuel, "Powers in nonsinusoidal situations. A review of definitions and physical meaning," *IEEE Trans. Power Del.*, vol. 5, no. 3, pp. 1377–1388, Jul. 1990.
- [5] A. E. Emanuel, *Power Definitions and the Physical Mechanism of Power Flow*. Hoboken, NJ: Wiley/IEEE, 2010.
- [6] L. S. Czarnecki, *Energy Flow and Power Phenomena in Electrical Circuits: Illusions and Reality Electrical Engineering*. Berlin, Germany: Springer-Verlag, 2000, vol. 82, pp. 119–126.
- [7] J. L. Willems, "Reflections on apparent power and power factor in nonsinusoidal and polyphase situations," *IEEE Trans. Power Del.*, vol. 19, no. 2, pp. 835–840, Apr. 2004.
- [8] P. E. Sutherland, "On the definition of power in an electrical system," *IEEE Trans. Power Del.*, vol. 22, no. 2, pp. 1100–1107, Apr. 2007.
- [9] A. E. Emanuel, "Poynting vector and the physical meaning of nonactive powers," *IEEE Trans. Instrum. Meas.*, vol. 54, no. 4, pp. 1457–1462, Aug. 2005.
- [10] L. S. Czarnecki, "Could power properties of three-phase systems be described in terms of the Poynting vector?," *IEEE Trans. Power Del.*, vol. 21, no. 1, pp. 339–344, Jan. 2006.
- [11] F. de León and J. Cohen, "Discussion of could power properties of three-phase systems be described in terms of the Poynting vector?," *IEEE Trans. Power Del.*, vol. 22, no. 2, pp. 1265–1266, Apr. 2007.
- [12] A. E. Emanuel, "About the rejection of Poynting vector in power system analysis," *Elect. Power Qual. Utilisation, J.*, vol. XIII, no. 1, pp. 43–49, 2007.
- [13] C. Steinmetz, *Theory and Calculation of Alternating Current Phenomena*. New York: W. J. Johnston, 1897.
- [14] J. H. Poynting, "On the transfer of energy in electromagnetic field," *Philosoph. Trans. Roy. Soc. London*, vol. 175, pp. 343–361.
- [15] R. M. Bozorth, *Ferromagnetism*. Hoboken, NJ: Wiley, 2003.
- [16] Development Coordination Group of EMTP, ver. EMTP-RV Electromagnetic Transients Program, 2012. [Online]. Available: <http://www.emtp.com>.

**Francisco de León** (S'86–M'92–SM'02) received the B.Sc. and the M.Sc. (Hons.) degrees in electrical engineering from the National Polytechnic Institute, Mexico City, Mexico, in 1983 and 1986, respectively, and the Ph.D. degree from the University of Toronto, Toronto, ON, Canada, in 1992.

He has held several academic positions in Mexico and has worked for the Canadian electric industry. Currently, he is an Associate Professor at the Polytechnic Institute of New York University, Brooklyn, NY. His research interests include the analysis of power definitions under nonsinusoidal conditions, the transient and steady-state analyses of power systems, the thermal rating of cables and transformers, and the calculation of electromagnetic fields applied to machine design and modeling.

**Layth Qaseer** received the B.Sc., M.Sc., and Ph.D. degrees in electrical engineering from the University of Baghdad, Baghdad, Iraq, in 1979, 1993, and 2004, respectively.

From 1979 to 2001, he was with the National Scientific Research Center and the Ministry of Industry. In 2005, he joined the Al-Khwarizmi College of Engineering, University of Baghdad, Baghdad. Currently, he is on a sabbatical leave from the Polytechnic Institute of New York University, Brooklyn, NY. His research interests include rotary, flat-linear, tubular-linear, and helical motion induction motors as well as induction heating systems.

**José Cohen** was born in Buenos Aires, Argentina, in 1951. He received the B.Sc. degree in electronic engineering from Instituto Politécnico Nacional, México City, México, in 1983, and the M.Sc. and Ph.D. degrees from Universidad Nacional Autónoma de México (UNAM), México City, México, in 1990 and 1999, respectively.

Currently, he is a Professor in the School of Engineering, UNAM. His main interests are in power electronics, clean energy, and electronic instrumentation.